Am J Transl Res 2026;18(3):2365-2379
www.ajtr.org /ISSN:1943-8141/AJTR0170578

Original Article

Remimazolam impairs bone marrow mesenchymal stem cell function and attenuates the tumor-promoting ability

Yan Yu[1,2*], Ting Liu[1*], Zhengsong Gu[2], Jin Wu[3], Wei Zhu[1]

[1]Department of Laboratory Medicine, School of Medicine, Jiangsu University, Zhenjiang 212013, Jiangsu, China; [2]Department of Anesthesiology, Zhenjiang Hospital of Traditional Chinese Medicine, Zhenjiang 212003, Jiangsu, China; [3]Department of Anesthesiology, Affiliated Hospital of Jiangsu University, Zhenjiang 212001, Jiangsu, China. [*]Equal contributors.

Received December 7, 2025; Accepted February 3, 2026; Epub March 15, 2026; Published March 30, 2026

Abstract: Bone marrow mesenchymal stem cells (BMMSCs) possess the potential for multidirectional differentiation and are involved in tissue regeneration, repair, and tumor progression. Remimazolam is a novel ultra-short-acting intravenous benzodiazepine sedative used for general anesthesia and procedural sedation. Propofol is a commonly applied intravenous anesthetic in clinical practice, featuring a rapid onset, short duration of action, and quick recovery. It has been reported that propofol exerts adverse effects on stem cell functions, yet few studies have compared the two agents for general anesthesia induction. Therefore, we aimed not only to evaluate the inhibitory effects of remimazolam and propofol on BMMSC biological functions but also to compare their relative impacts on BMMSC proliferation, migration, stemness, and subsequent tumor-promoting capacity in vitro. CCK-8 cell viability and colony formation assays were performed to detect BMMSC proliferation. Adipogenic and osteogenic differentiation assays were used to assess the multidirectional differentiation potential of BMMSCs. Additionally, network pharmacology analysis was employed to explore the common target genes of remimazolam and propofol and their associated signaling pathways. The effects of conditioned medium from BMMSCs treated with remimazolam or propofol on gastric cancer cell lines were investigated using transwell assays, flow cytometry, and western blot. The results showed that remimazolam inhibited the proliferation and migration of BMMSCs, suppressed osteogenic differentiation, promoted adipogenic differentiation, and reduced the stemness of BMMSCs. Compared with propofol treatment, remimazolam exerted a less pronounced inhibitory effects on these biological processes of BMMSCs. Network pharmacology analysis revealed that remimazolam modulates the paracrine level of the cytokine IL-8 mainly through the PI3K/AKT pathway. Furthermore, remimazolam further attenuated the tumor-promoting effect of BMMSCs on gastric cancer cells. In conclusion, remimazolam exerts stronger inhibitory effects on the stemness and paracrine function of BMMSCs than propofol, thereby reducing their tumor-promoting capacity to a greater extent. Our study focuses on remimazolam and provides experimental evidence for the rational clinical application of anesthetics.

Keywords: Remimazolam, propofol, mesenchymal stem cells, gastric cancer

Introduction

BMMSCs are resident stromal cells present in nearly all tissues, including the heart, where they play a pivotal role in tissue regeneration and repair [1]. MSCs have been extensively exploited for tissue engineering and cell replacement therapies, owing to their inherent capacity for multidirectional differentiation [2-5]. In recent years, numerous studies have also investigated the functional role of MSCs in tumor progression [6, 7], a process in which the paracrine secretion of various cytokines is known to exert a critical regulatory effect [8, 9]. Given the promising clinical potential of MSCs, any damage to these cells or impairment of their biological functions is likely to compromise tissue regenerative capacity. Correspondingly, elucidating the factors that modulate the tumor-promoting properties of MSCs is of great translational significance for both basic research and clinical practice.

https://doi.org/10.62347/G0BJ9420

Remimazolam is an ultra-short-acting benzodiazepine sedative-anesthetic approved for clinical use in general anesthesia induction, maintenance, and procedural sedation [10]. Multiple studies have validated the efficacy and safety of remimazolam for general anesthesia and sedative procedures [11]. By contrast, propofol remains the first-line agent for total intravenous anesthesia, attributed to its predictable onset, rapid and consistent recovery profile, as well as favorable safety and efficacy profiles. Accumulating evidence indicates that anesthetics can modulate the differentiation of mesenchymal stem cells (MSCs) [12, 13]. For instance, BMMSCs have been induced to differentiate into neural-like cells to facilitate the repair of injured spinal cords [14]. Recent clinical trials have also compared the effects of these two agents on psychomotor function recovery [15, 16]. However, the impacts of remimazolam and propofol on the biological functions of BMMSCs remain poorly elucidated. Given the widespread clinical use of both anesthetics and the critical role of BMMSCs in tumor progression, the present study aimed not only to assess whether remimazolam and propofol can inhibit BMMSC biological functions but also to compare their relative inhibitory impacts on BMMSCs and their tumor-promoting capacity. We further explored the underlying molecular mechanisms to provide an experimental basis for the rational clinical administration of these two commonly used anesthetics.

Materials and methods

Cell culture

Healthy donor-derived bone marrow was collected in a heparin anticoagulant tube at the Affiliated Hospital of Jiangsu University, and all protocols were approved by the local ethics committee of the Affiliated Hospital of Jiangsu University, China. The collected bone marrow was slowly added to a centrifuge tube with an equal volume of PBS along the tube wall and gently blown and mixed. Bone marrow fluid diluted in PBS was slowly added to 1.077 g/mL Ficoll, the human lymphocyte separation solution, along the tube wall. The centrifuge was set to slow rise and drop, 800 g, and centrifuged for 20 min. BMMSCs are found in the tunica albuginea layer in the interface between the plasma and separation solution. The white membrane layer was mixed into PBS and then rinsed. Cells were resuspended in α-MEM nutrient solution containing 10% FBS. The human gastric cancer cell line HGC-27 was purchased from the Cell Bank of Type Culture Collection of the Chinese Academy of Sciences and then cultured in RPMI 1640 medium (Biological Industries, USA) supplied with 10% FBS. All cells were maintained at 37°C in a humidified atmosphere of 5% CO_2.

Flow cytometry

The ALDH activity was assayed using the ALDEFLUOR Kit and following the manufacturer's instructions (Stemcell, Canada). Diethylaminobenzaldehyde (DEAB) was added to each sample as a negative control.

Cell viability assay

We performed the Cell Count Kit-8 assays to assess the potential effects of assessing the half-maximal inhibitory concentration of propofol and Remimazolam. Following the instructions, the BMMSCs were pre-treated with propofol and Remimazolam for 48 h. Cells were seeded into 96-well plates at a density of 2 × 10^3 per well and incubated overnight at 37°C in 5% CO_2. Subsequently, 10 μL of the CCK-8 solution and 90 μL of fresh complete medium were added to each well. Absorbance values at 450 nm were measured.

Adipogenic and osteogenic differentiation of BMMSCs

BMMSCs treated with propofol and remimazolam were cultured in six-well plates. When the confluence of the bottom cells reached 85%, the discarded medium was replaced with adipogenic differentiation medium or osteogenic differentiation medium and continued in the incubator at 37°C, 5% CO_2. Subsequently, the adipogenic differentiation medium and osteogenic differentiation medium were changed every three days. The evolution of cell morphology was observed simultaneously by microscopy. The culture phase was terminated until lipid droplet formation was visible inside the cells, and the oil red O staining procedure was performed. The osteogenic differentiation medium was changed every three days, and the culture was stopped for 18 days for alizarin red S staining.

Colony formation assay

BMMSCs treated with propofol and remimazolam in the six-well plate were centrifuged by trypsin digestion. After collecting cells, the cells were resuspended in 1 mL PBS and counted. A total of 1,500 cells, in three duplicate groups, from the counted cells, were inoculated into Corning 35 mm with 2 mL of culture medium in cell culture dishes. The change was observed every three days, and the clonal morphology was observed for 10-14 days, which terminated when cells were grouped. Small dishes were washed with PBS, fixed with 4% paraformaldehyde at 4°C for half an hour, and residual paraformaldehyde was removed in PBS. The cells were stained with crystal violet for 15 min. The crystal violet dye solution was recovered, the residual crystal violet was removed with PBS, and the number of clones was photographed.

Western blot

Cell proteins were extracted on ice using a Total protein extraction kit (Keygen Technology, China). After determining protein concentration, 20 μg of total protein from each sample was separated with 10% sodium dodecyl sulfate-polyacrylamide gel electrophoresis and then transferred to polyvinylidene fluoride membranes (Millipore, Billerica, MA, USA). The PVDF membranes were incubated with primary antibodies at 4°C overnight after blocking with 5% skim milk for 1 hour and washed with TBST three times, 5 min each. Then, membranes were incubated with secondary antibodies at 37°C for 1 h. Finally, the blots were visualized using the enhanced chemiluminescent detection system (Millipore, Billerica, MA, USA) and analyzed using Image-Pro Plus version 5.1 (Media Cybernetics Inc, Rockville, MD, USA). Sources of primary antibodies were shown as follows: anti-C-MYC, NANOG, SOX2, SALL4, BAX, P-AKT, T-AKT (1:1000, Cell Signaling Technology, USA), CTCF (1:1,000, Abcam, UK), CD44 (1:1000, Wanleibio, CHINA), BCL-2 (1:1000, R&D Systems, USA), β-actin (1:4,000, Cell Signaling Technology, USA). The secondary antibodies used in the study were goat anti-mouse and anti-rabbit secondary antibodies (both diluted to 1:3,000, Cell Signaling Technology, USA) conjugated with horseradish peroxidase.

Quantitative real-time reverse transcription-polymerase chain reaction (qRT-PCR)

Total RNA was isolated using Trizol reagent (Ambion) from BMMSCs under different treatments of propofol and remimazolam. Quantitative reverse transcription PCR (qRT-PCR) was performed using Ultra SYBR (CWBIO, China) according to the manufacturer's instructions. The primer sequences used in the study are as follows: PPAR-γ (forward: 5'-GCCTGCATTTCTGCATTCTG-3', reverse: 5'-CACGGAGCTGATCCCAAAG-3'); OPN (forward: 5'-CAGTTGTCCCCACAGTAGACAC-3', reverse: 5'-GTGATGTCCTCGTCTGTAGCATC-3'); ALP (forward: 5'-GCCATTGGCACCTGCCTTAC-3', reverse: 5'-AGCTCCAGGGCATATTTCAGT-3'); RUNX2 (forward: 5'-CACTGGCGCTGCAACAAGA-3', reverse: 5'-CATTCCGGAGCTCAGCAGAATAA-3').

Network pharmacology analysis

The linear representation of the 2D structure and Canonical SMILES chemical structure for propofol and remimazolam were downloaded from the PubChem database (https://pubchem.ncbi.nlm.nih.gov/). The propofol and remimazolam-related target genes were predicted from the Super-PRED database (https://prediction.charite.de/). The KEGG pathway analysis and HALLMARK analysis of common targets were performed in SangerBox software (http://sangerbox.com/).

Sphere formation assay

First, 2×10^3 GC cells were cultured in serum-free RPMI-1640 containing EGF (20 ng/mL, PeproTech, USA), b-FGF (20 ng/mL, PeproTech), and B27 (2%, BD Biosciences, USA) and then plated in six-well ultralow attachment plates (Corning). After 10 days, the formed spheres were imaged using a phase-contrast microscope.

Transwell migration and invasion assay

To detect the tumor-promoting ability of BMMSCs, HGC-27 cells were pre-treated with BMMSCs-CM, 5×10^4 HGC-27 were suspended in 200 μL of serum-free RPMI-1640 and seeded in the upper compartment of transwell filters with 8 μm pores (Corning, USA). RPMI-1640 containing 10% FBS was added to the bottom well to allow cell migration following the con-

centration difference. After incubation for 16 h, the migrated cells were fixed for 15 min using 4% paraformaldehyde (Hushi, China), stained with crystal violet, and visualized at 200 × with the inverted biological microscope. In the invasion experiment, Matrigel was spread in the supramembrane compartment. Next, 6×10^4 HGC-27 cells suspended in 200 μL serum-free RPMI-1640 were spread in the upper chamber of Transwell. RPMI-1640 containing 10% FBS was added to the bottom well to allow cell migration following the concentration difference. After 8 hours, we used a cotton swab to remove the cells that did not migrate. Migrated cells were fixed with 4% formaldehyde for 30 min and then photographed and counted in three random fields for each well under the microscope (Nikon).

Cell cycle analysis

A total of 1×10^5 cells per well were seeded into six-well plates, incubated overnight, and then treated with Pro-BMMSCs-CM and Rem-BMMSCs-CM. After 48 h, 1×10^6 cells per well were collected by centrifugation and stained with propidium iodide in PBS for 30 min at 4°C in the dark before being analyzed with flow cytometry.

Statistical analysis

GraphPad Prism (version 7.02) was employed for statistical analyses. Data is presented as means ± standard deviation (SD). The variance was similar between the groups being compared. Statistical significance was calculated using the Student's t-test or one-way analysis of variance. $P < 0.05$ was considered to be statistically significant.

Results

Inhibition of propofol and remimazolam on the cell viability of BMMSCs

Mesenchymal stem cells isolated and cultured from bone marrow tissue exhibited positive expression of mesenchymal markers (CD90, CD105, CD29) and negative expression of hematopoietic markers (CD45, CD34, CD19). We evaluated the effects of propofol and remimazolam on BMMSC viability. Both anesthetics induced a reduction in BMMSC viability, with propofol exerting a significant dose-dependent inhibitory effect compared to the control group. Similarly, remimazolam treatment resulted in a significant decrease in BMMSC viability following 48 h of exposure (**Figure 1A**, **1B**). Based on these viability data, we selected 500 μg/mL propofol and 300 μg/mL remimazolam for all subsequent experiments. We further observed the morphological changes of BMMSCs after anesthetic treatment: compared with control cells, propofol-treated BMMSCs exhibited typical apoptotic features, including membrane blebbing and cytoplasmic contraction (**Figure 1C**). In contrast, remimazolam-treated BMMSCs maintained a spindle-shaped, fibroblast-like morphology with firm adherence to the culture substrate, which was analogous to the growth phenotype of normal BMMSCs.

The effect of propofol and remimazolam on the differentiation potential of BMMSCs

Due to the multidirectional differentiation potential of MSCs, we performed the adipogenic or osteogenic differentiation of BMMSCs in the presence of a specific differentiation medium. The results showed a significant decrease in the adipogenic and osteogenic differentiation of BMMSCs treated with propofol and remimazolam (**Figure 2A**, **2B**). We also found that this inhibition was more pronounced after co-treatment with these two anesthetics. The expression of osteogenesis-related gene (ALP, OPN, RUNX2) and adiponectin-related gene (PPAR-γ) was also significantly decreased (**Figure 2C**).

Propofol and remimazolam inhibit the proliferation, migration, and stemness of BMMSCs

We performed a colony formation assay to evaluate the self-proliferative capacity of BMMSCs treated with propofol or remimazolam. Compared with the control group, BMMSCs treated with either anesthetic exhibited significantly reduced self-proliferative potential (**Figure 3A**). Additionally, the Transwell migration assay demonstrated a marked decrease in the migratory capacity of BMMSCs following treatment with both anesthetics (**Figure 3B**, **3C**). Western blot analysis was employed to detect changes in the expression levels of stemness-related transcription factors in BMMSCs; the results showed that both propofol and remimazolam significantly downregulated the expression of stemness transcription factors, including SOX2 and NANOG. Moreover, the expression levels of stemness-associated markers CD44 and

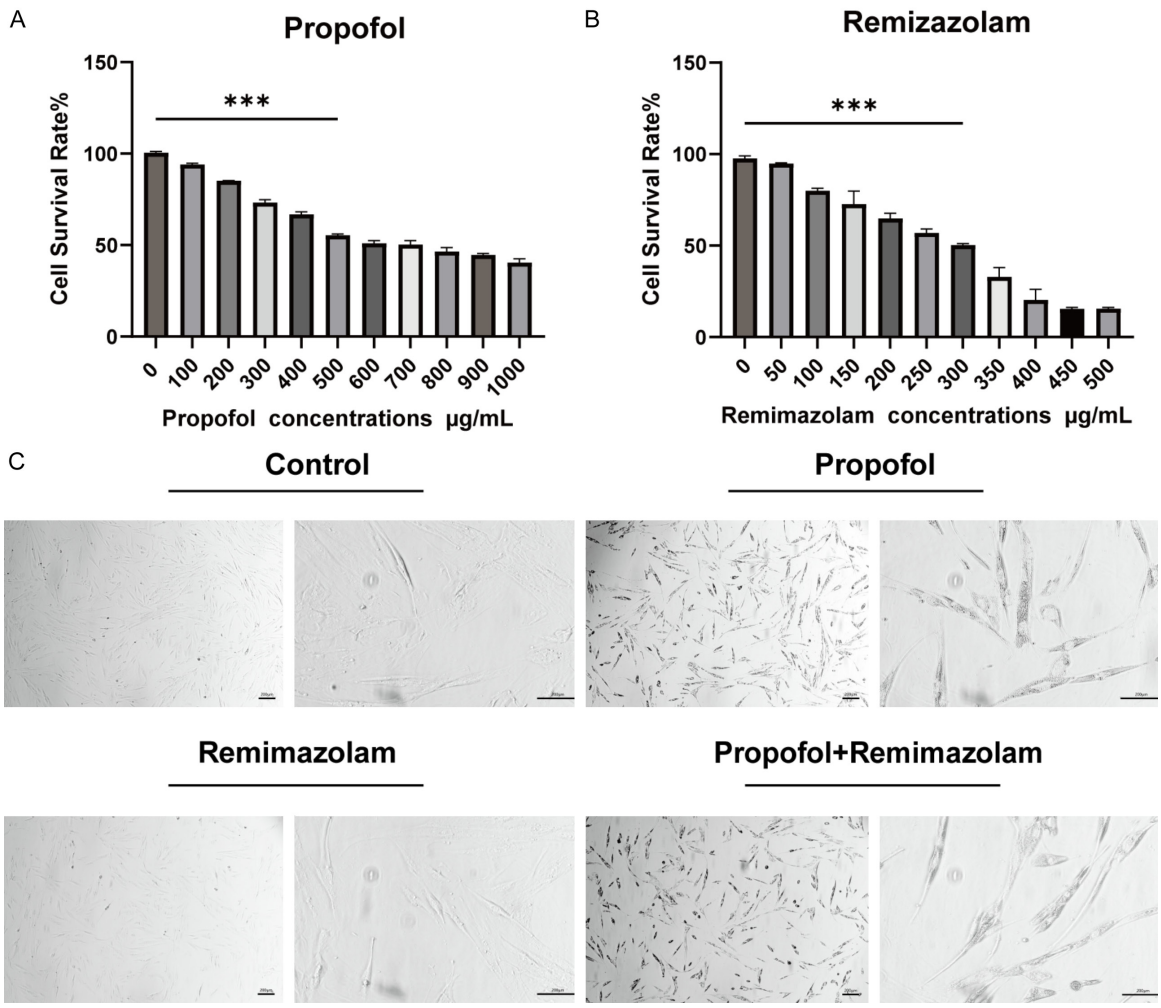

Figure 1. Inhibition of propofol and remimazolam on cell viability of BMMSCs. A, B. Cultured BMMSCs were treated with various concentrations of propofol or remimazolam for 48 h. Cell viability was assessed using the CCK-8 assay, with the absorbance of each well measured at 450 nm. The relative absorbance value of the control group was set as 100% (used as the reference). Significant differences between the control and the group treated with propofol and remimazolam. C. Effects of propofol and remimazolam on the morphological characteristics of BMMSCs. BMMSCs were seeded in 96-well plates and treated with 500 μg/mL propofol or 300 μg/mL remimazolam for 48 h. Morphological changes were observed under a light microscope. Quantitative statistics are shown as means ± SD. ****P < 0.001*.

c-MYC were also significantly decreased (**Figure 3D**). Notably, compared with propofol treatment, remimazolam exerted a less pronounced inhibitory effect on BMMSC proliferation, migration, and stemness maintenance.

Propofol and remimazolam function on BMMSCs via the PI3K/AKT pathway

A total of 79 potential targets for propofol and 96 potential targets for remimazolam were retrieved from public databases. Data analysis was performed using Sangerbox software (**Figure 4A**). Subsequently, 40 common targets were identified, and these common targets were subjected to KEGG signaling pathway enrichment analysis and HALLMARK pathway analysis (**Figure 4B**, **4C**). The enrichment results indicated that the PI3K/AKT signaling pathway was the most closely associated pathway with the common targets. Consistent with this in silico finding, Western blot analysis demonstrated a reduction in AKT phosphorylation levels in BMMSCs following 48 h of treatment with propofol or remimazolam (**Figure 4D**). Given that BMMSCs exert their biological functions primarily through paracrine secretion, we further detected the level of IL-8. The

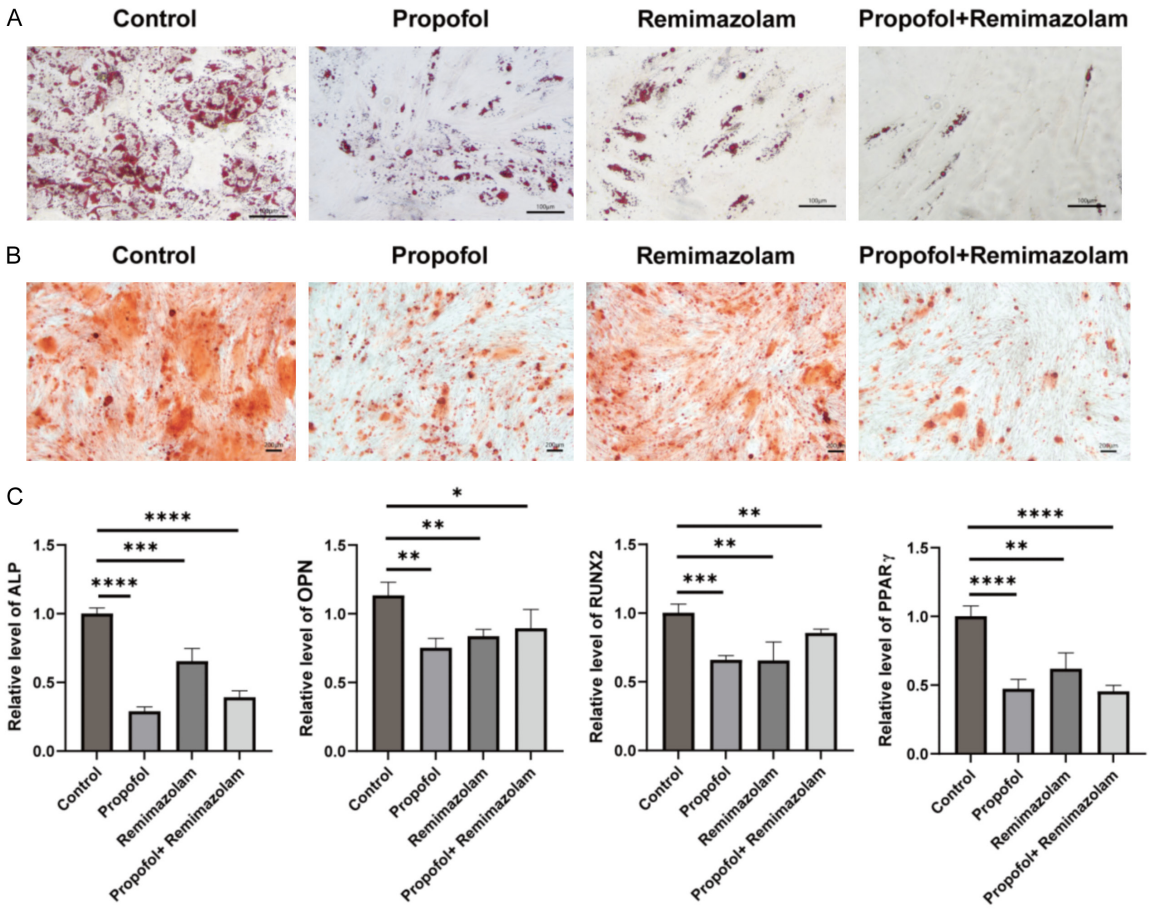

Figure 2. The effect of propofol and Remimazolam on the differentiation potential of BMMSCs. A, B. BMMSCs were cultured at 500 μg/mL propofol and 300 μg/mL remimazolam with adipogenic or osteogenic differentiation medium. After adipogenic differentiation culture for 2 weeks or after osteogenic differentiation for 3 weeks, the cells were fixed and stained with oil red O (adipogenic differentiation) or alizarin red S (osteogenic differentiation). C. Cells cultured after adipogenic and osteogenic differentiation were collected and subjected to quantitative real-time PCR to detect the osteoblast markers *ALP, OPN,* and *RUNX 2,* as well as the adipocyte marker *PPAR-γ*. Quantitative statistics are shown as means ± SD. **P < 0.05, **P < 0.01, ***P < 0.001, ****P < 0.0001*.

results showed that propofol and remimazolam treatment significantly downregulated IL-8 secretion in BMMSCs. Additionally, quantitative analysis revealed that the mRNA expression level of IL-8 was also significantly decreased in treated BMMSCs compared to the control group (**Figure 4E**, **4F**).

BMMSCs treated with propofol and remimazolam inhibited gastric cancer cell proliferation, migration, and invasion in vitro

Accumulating evidence has demonstrated that tumor-recruited MSCs promote metastasis and enhance the proliferation and migration of gastric cancer cell lines [17, 18]. Therefore, we further investigated the effects of propofol and remimazolam on the tumor-promoting capacity of BMMSCs. The conditioned medium (CM) was collected from BMMSCs treated with propofol or remimazolam (designated as Pro-BMMSCs-CM and Rem-BMMSCs-CM, respectively), and this CM was subsequently used to treat gastric cancer cells to evaluate changes in their proliferation, migration, and invasion. Colony formation and cell proliferation assays showed that HGC-27 cells treated with Pro-BMMSCs-CM or Rem-BMMSCs-CM exhibited significantly reduced proliferative capacity; notably, the tumor-promoting effect of BMMSCs on HGC-27 cells' growth was more markedly attenuated when BMMSCs were co-treated with both anesthetics (**Figure 5A**, **5B**). Additionally, the migratory ability of gastric cancer cells was significantly decreased following treatment with Pro-

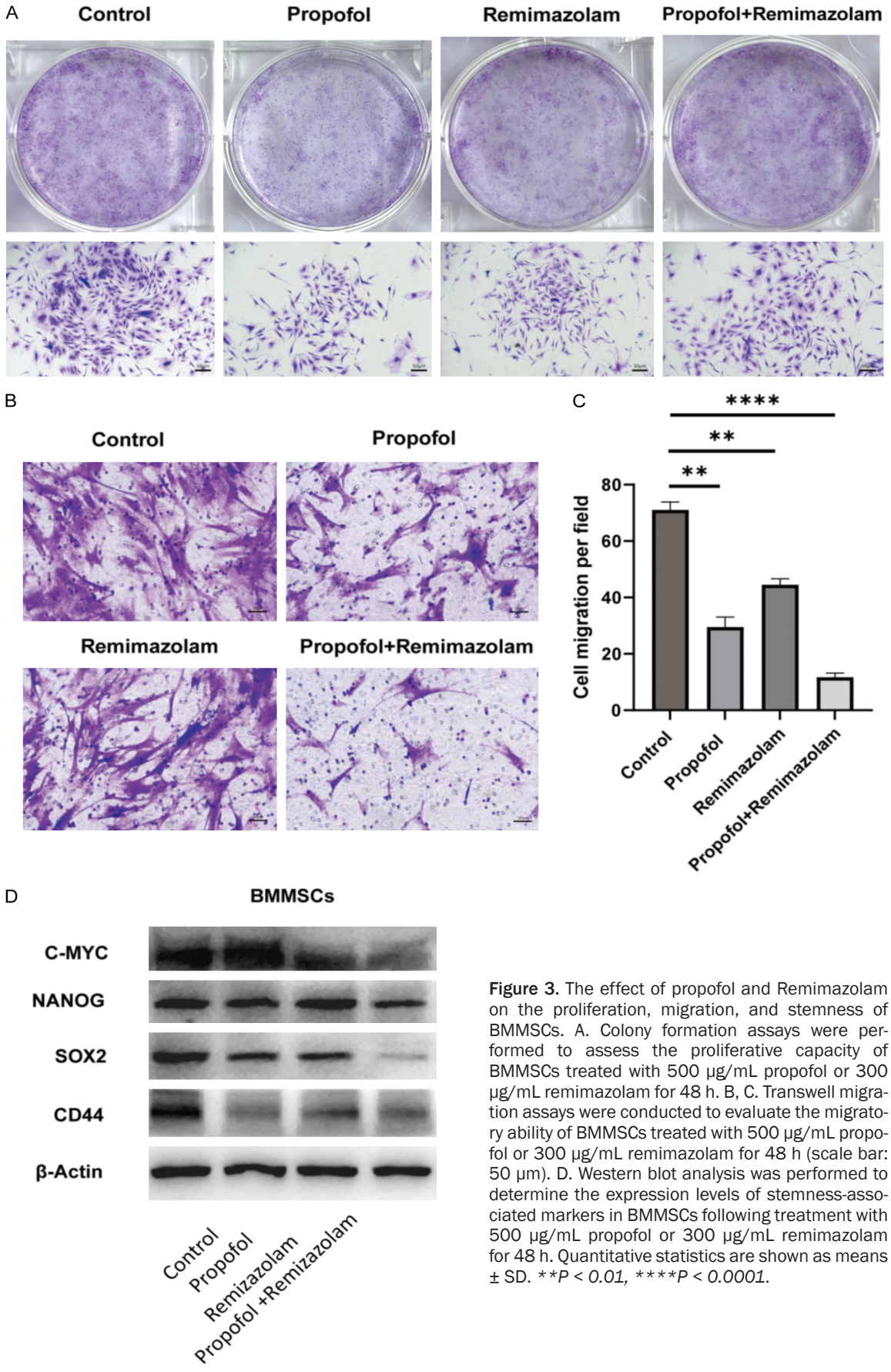

Figure 3. The effect of propofol and Remimazolam on the proliferation, migration, and stemness of BMMSCs. A. Colony formation assays were performed to assess the proliferative capacity of BMMSCs treated with 500 μg/mL propofol or 300 μg/mL remimazolam for 48 h. B, C. Transwell migration assays were conducted to evaluate the migratory ability of BMMSCs treated with 500 μg/mL propofol or 300 μg/mL remimazolam for 48 h (scale bar: 50 μm). D. Western blot analysis was performed to determine the expression levels of stemness-associated markers in BMMSCs following treatment with 500 μg/mL propofol or 300 μg/mL remimazolam for 48 h. Quantitative statistics are shown as means ± SD. ***P < 0.01, ****P < 0.0001*.

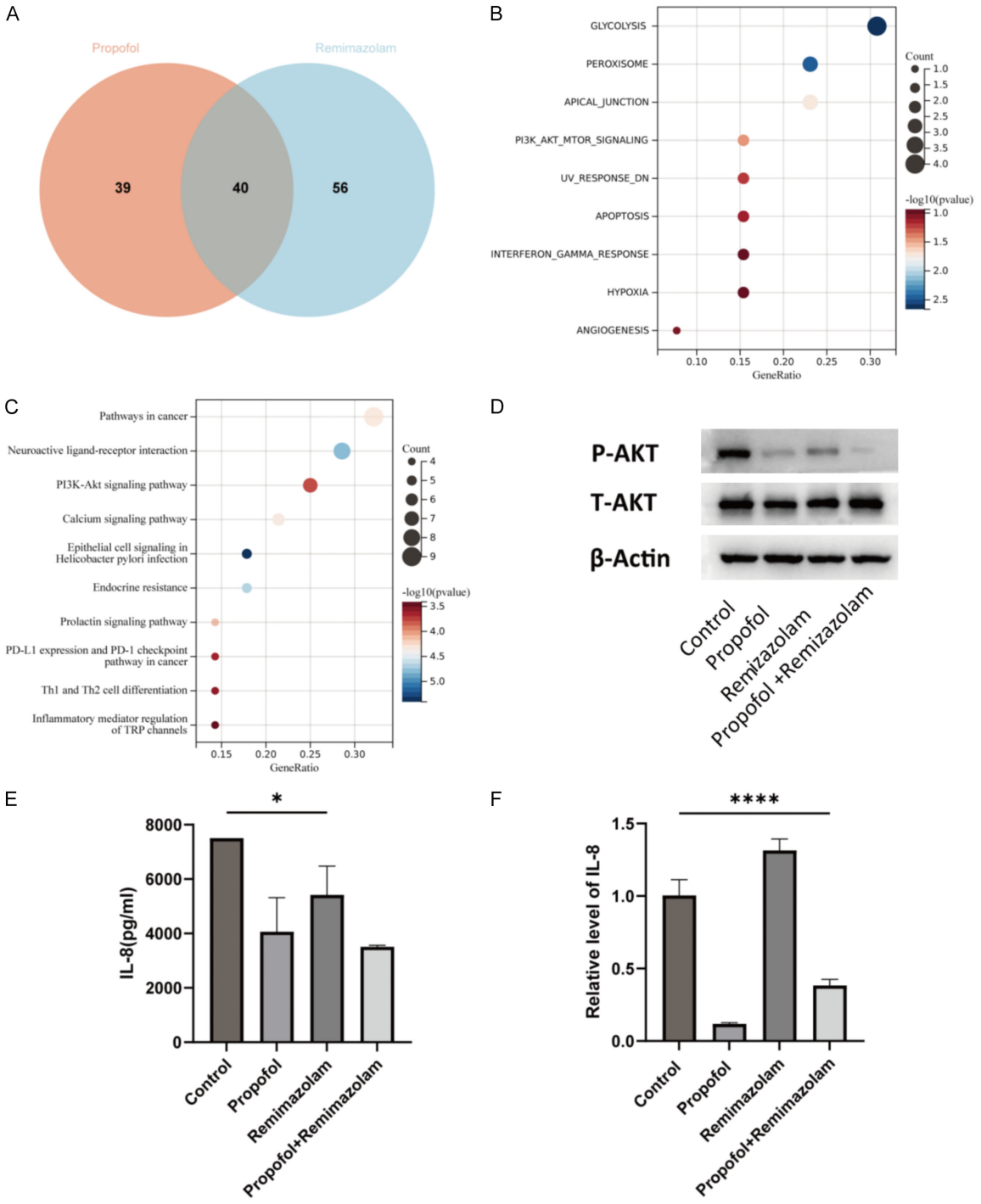

Figure 4. Propofol and Remimazolam function on BMMSCs via the PI3K/AKT pathway. A. Wayn showed targets for propofol and remimazolam collected from databases. B, C. KEGG pathway enrichments and HALLMARK analysis with the common target gene clustered in propofol and remimazolam. D. Western blot was performed to detect the change of AKT in BMMSCs. E, F. The levels of IL-8 protein and mRNA in the culture supernatant of BMMSCs were measured. Quantitative statistics are shown as means ± SD. **P < 0.05, ****P < 0.0001*.

BMMSCs-CM or Rem-BMMSCs-CM (**Figure 5C**, **5D**). Consistent with these findings, the transwell invasion assay yielded similar results, showing a significant reduction in the invasive capacity of gastric cancer cells. Collectively, these results indicate that propofol and remimazolam can impair the tumor-promoting ability of BMMSCs (**Figure 5E**, **5F**).

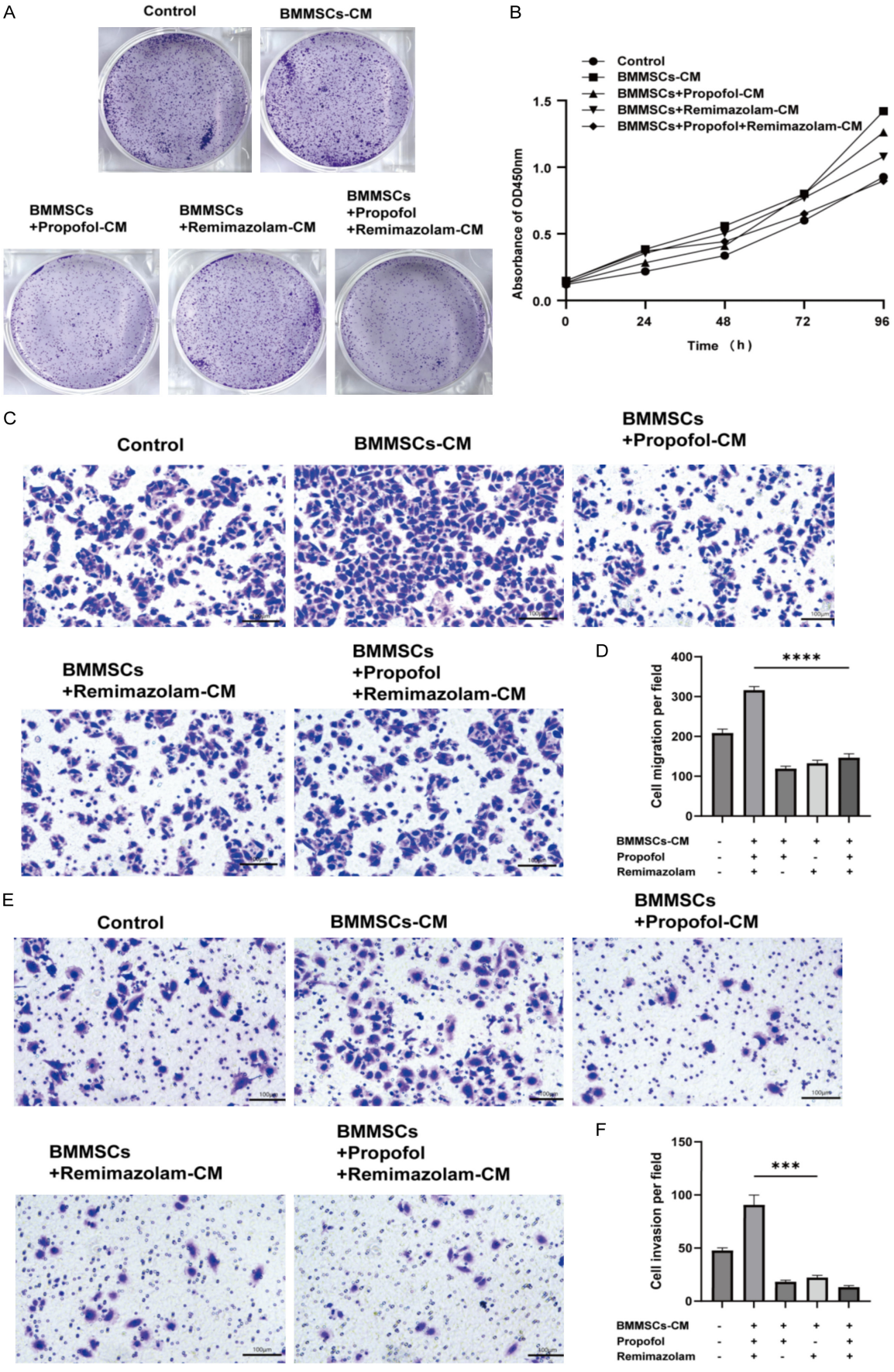
A
Control
BMMSCs-CM
BMMSCs +Propofol-CM
BMMSCs +Remimazolam-CM
BMMSCs +Propofol +Remimazolam-CM
B
Control
BMMSCs-CM
BMMSCs+Propofol-CM
BMMSCs+Remimazolam-CM
BMMSCs+Propofol+Remimazolam-CM
Absorbance of OD450nm
Time (h)
C
Control
BMMSCs-CM
BMMSCs +Propofol-CM
BMMSCs +Remimazolam-CM
BMMSCs +Propofol +Remimazolam-CM
D
Cell migration per field
****
BMMSCs-CM
Propofol
Remimazolam
E
Control
BMMSCs-CM
BMMSCs +Propofol-CM
BMMSCs +Remimazolam-CM
BMMSCs +Propofol +Remimazolam-CM
F
Cell invasion per field
***
BMMSCs-CM
Propofol
Remimazolam

Figure 5. BMMSCs treated with propofol and remimazolam inhibited gastric cancer cell proliferation, migration, and invasion in vitro. A, B. The Colony formation assay and cell counting kit-8 assay were used to detect the proliferation of HGC-27 cells after being treated with BMMSCs-CM. C, D. Transwell migration (scale bar, 50 μm) assays were performed in HGC-27 following BMMSCs-CM treatment. E, F. Invasion (scale bar, 50 μm) assays were performed in HGC-27 following BCMSCs-CM treatment. Quantitative statistics are shown as means ± SD. ****P < 0.001, ****P < 0.0001*.

Propofol and remimazolam can weaken the effects of BMMSCs-CM on cell stemness and cycle progression in gastric cancer cells

We found that the sphere-forming capacity of HGC-27 gastric cancer cells was significantly reduced following treatment with Pro-BMMSCs-CM or Rem-BMMSCs-CM (**Figure 6A**, **6B**). Additionally, Pro-BMMSCs-CM and Rem-BMMSCs-CM treatment decreased ALDH activity in CSCs (**Figure 6C**). Moreover, the protein expression levels of the stemness-associated markers Sall4 and CTCF were downregulated in HGC-27 cells treated with these two conditioned media (**Figure 6D**). With respect to cell cycle distribution, Pro-BMMSCs-CM and Rem-BMMSCs-CM treatment slightly decreased the percentage of HGC-27 cells in the G1 phase from approximately 60% to 55%, though this change was not statistically significant. Furthermore, Western blot analysis demonstrated that Pro-BMMSCs-CM and Rem-BMMSCs-CM treatment reduced the expression of Bcl-2, a key anti-apoptotic protein that inhibits cell apoptosis (**Figure 6E**, **6F**).

Discussion

BMMSCs, which reside in nearly all tissues of the human body, participate in the repair of damaged tissues and exert immunosuppressive effects by modulating immune responses. These functional properties are attributed to their inherent capacity for multidirectional differentiation and the secretion of trophic factors. In addition, the role of BMMSCs in tumor progression has been extensively investigated [19-21]. Accumulating evidence indicates that hBMMSC-CM can upregulate c-Myc expression in gastric cancer cells, which may serve as a key driver of carcinogenesis.

Propofol, a traditional intravenous anesthetic, has been shown to affect the differentiation capacity of stem cells, as well as other biological processes such as nerve regeneration and spinal cord injury repair. Remimazolam, a novel reversible ultra-short-acting benzodiazepine, exerts sedative effects as a positive allosteric modulator of the γ-aminobutyric acid type A (GABAA) receptor [22]. Its high water solubility and metabolism by tissue esterases enable rapid induction of sedative anesthesia [23]. Compared with other similar intravenous sedatives, remimazolam exhibits advantages including rapid onset, short recovery time, favorable cardiopulmonary safety, and excellent pharmacokinetic profiles. Currently, remimazolam has been approved for clinical use in anesthesia, and numerous experimental studies have demonstrated that it can achieve effective and safe anesthetic effects when administered alone or in combination with other agents [24]. Propofol, as a conventional intravenous anesthetic, has been widely used for the induction and maintenance of clinical anesthesia [25]. Several clinical trials and studies have compared these two anesthetics in terms of psychomotor function, hemodynamic parameters, and post-anesthetic recovery [26, 27]. Moreover, researchers have focused on the role of propofol in tumor progression [28]. However, there is a paucity of research regarding the effects of remimazolam on tumor biology. In the present study, we mainly investigated the biological impacts of remimazolam (a novel anesthetic) and propofol (a traditional anesthetic) on BMMSCs, and further explored the underlying molecular mechanisms. This work aims to provide experimental evidence to support the rational clinical application of these anesthetics.

BMMSCs were isolated from fresh clinical bone marrow samples and cultured in vitro. Flow cytometry analysis was performed to characterize their surface marker profile, confirming the phenotypic identity of the isolated cells. Cell viability assays demonstrated that remimazolam and propofol inhibited BMMSC viability in a concentration-dependent manner. Under light microscopy, both anesthetics were observed to induce membrane blebbing and cytoplasmic shrinkage in BMMSCs-morphological features suggestive of cell death-indicating that these two drugs may trigger BMMSC death at high concentrations [29]. Given that multidi-

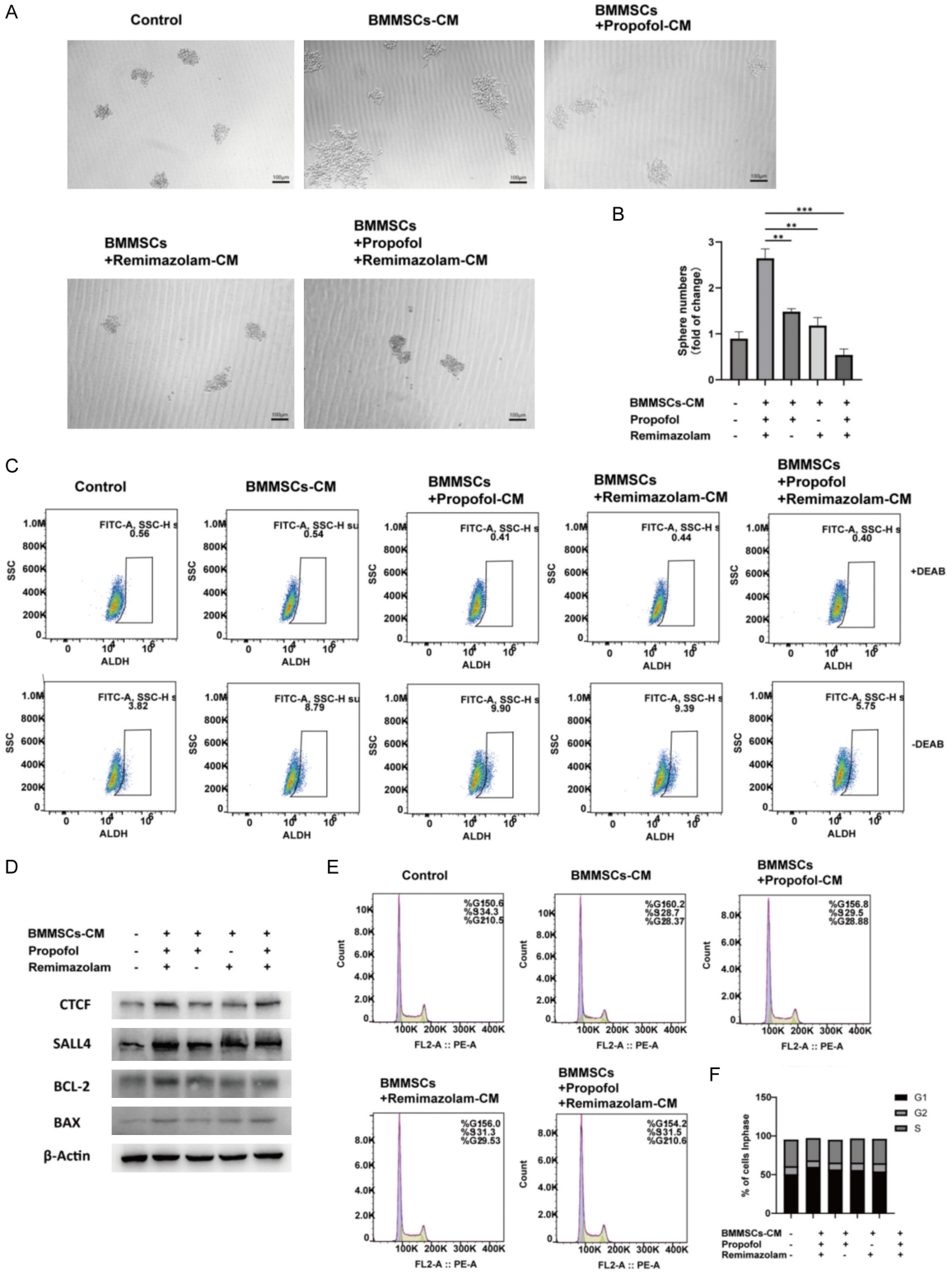

Figure 6. Propofol and Remimazolam can weaken the effects of BMMSCs-CM on cell stemness and cycle progression in gastric cancer cells. A, B. Sphere formation (scale bar, 200 μm) assays were performed in HGC-27 following BMMSCs-CM treatment. C. The ALDH activity of HGC-27 was tested by ALDEFLUOR analyses. Propofol and remimazolam were added to BMMSCs-CM and incubated at room temperature for 1 h earlier. D. Western blotting was performed to determine the expression of Bcl-2 and Bax in HGC-27 cells. E, F. The changes in cell cycle distribution were not significant after three experiments. Quantitative statistics are shown as means ± SD. **P < 0.01, ***P < 0.001.

rectional differentiation capacity is a core characteristic of BMMSCs, we evaluated their adipogenic and osteogenic differentiation potential via in vitro induction with lineage-specific differentiation media [30]. Staining results revealed that propofol exerted a more potent inhibitory effect on BMMSC differentiation than remimazolam; notably, the inhibitory effect was most pronounced when BMMSCs were co-treated with both anesthetics. Consistent with these phenotypic observations, RT-qPCR assays showed that the expression levels of adipogenesis- and osteogenesis-related genes were significantly downregulated following anesthetic treatment, with the most prominent inhibition observed in the combined treatment group. It has been reported that BMMSCs can be recruited to tumor sites, where they are educated by the tumor microenvironment to promote tumor growth. To explore the effects of remimazolam and propofol on BMMSC migratory capacity, we performed Transwell migration assays. The results indicated that BMMSC migration was substantially inhibited when the two drugs were administered in combination. The ability to maintain self-renewal and multidirectional differentiation is a hallmark of BMMSC stemness [31]. Western blot analysis was therefore conducted to assess the expression of stemness-associated markers in BMMSCs. Similarly, the most significant reduction in stemness-related markers was observed in BMMSCs co-treated with both anesthetics.

Network pharmacology analysis identified the PI3K/AKT signaling pathway as a common target pathway of remimazolam and propofol. The PI3K/AKT signaling pathway regulates the function of multiple downstream substrates and is involved in mediating cell survival, cell cycle progression, and cell proliferation, thereby playing a critical role in carcinogenesis [32-34]. Western blot analysis was further performed to verify this finding, demonstrating that remimazolam combined with propofol impaired the phosphorylation level of AKT in BMMSCs. Collectively, these results indicate that the combination of remimazolam and propofol inhibits BMMSC proliferation, migration, and stemness by targeting the PI3K/AKT signaling pathway. Previous studies have shown that hBMMSC-CM can promote tumor growth by upregulating c-MYC expression. Additionally, MSCs consistently secrete immunomodulatory molecules, IL-8, in response to inflammatory stimuli [35, 36]. IL-8, a pro-tumorigenic chemokine in the tumor microenvironment, can promote tumor cell proliferation and epithelial-mesenchymal transition [37]. ELISA results revealed that the secretion level of IL-8 in BMMSCs was markedly decreased following treatment with remimazolam or propofol. We therefore further explored the effects of these two anesthetics on the tumor-promoting capacity of BMMSCs, using the gastric cancer cell line HGC-27 as the in vitro model. Consistent with our hypothesis, remimazolam and propofol impaired the tumor-promoting capacity of BMMSCs, as evidenced by the significant reduction in the proliferative, migratory, and invasive capacities of HGC-27 cells treated with Pro-BMMSCs-CM or Rem-BMMSCs-CM. This phenomenon may be attributed to the downregulated secretion of IL-8 by BMMSCs. Notably, we also observed a marked alteration in the stemness of HGC-27 cells following treatment with BMMSC-derived conditioned media. Sphere formation assays, flow cytometry, and Western blot analysis collectively demonstrated that both remimazolam and propofol attenuated the tumor-promoting ability of BMMSCs by regulating the stemness of gastric cancer cells. Additionally, we investigated the effects of remimazolam and propofol on the apoptosis and cell cycle distribution of HGC-27 cells. Western blot results showed that BMMSC-CM treatment increased the expression of anti-apoptotic markers in HGC-27 cells; however, this upregulatory effect was reversed by treatment with Pro-BMMSC-CM or Rem-BMMSC-CM. In contrast, no significant changes in HGC-27 cell cycle distribution were observed following treatment with either conditioned medium [38]. In the present study, we demonstrated that remimazolam and propofol inhibit BMMSC proliferation, migration, and stemness by targeting the PI3K/AKT signaling pathway, with remimazolam exerting a less potent inhibitory effect on BMMSCs compared to propofol. Furthermore, the downregulated paracrine secretion of IL-8 by anesthetic-treated BMMSCs contributed to the attenuation of their tumor-promoting capacity. It should be acknowledged that this study has several limitations. Specifically, it should be noted that the design of this experimental group aims at the conceptual verification of

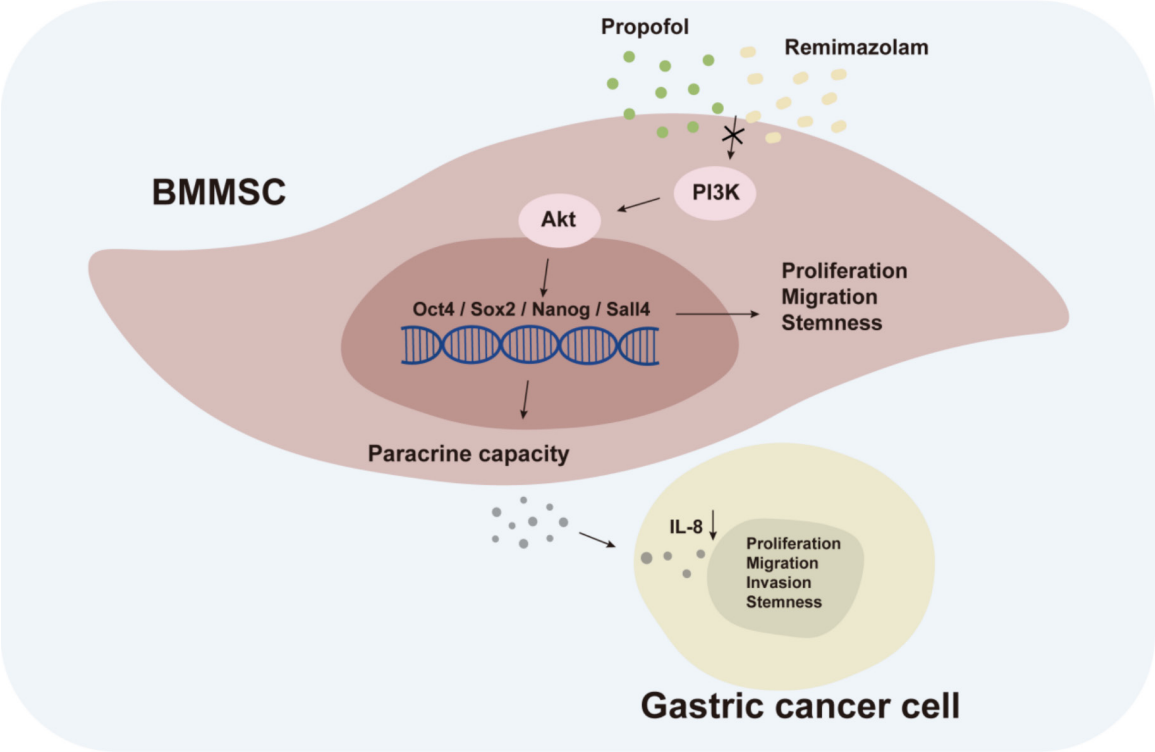

Figure 7. Schematic diagram.

the mechanism of action rather than the simulation of real-world clinical scenarios. Clinically, although remimazolam and propofol are widely used for surgical sedation and general anesthesia, they are rarely administered in a fixed combination in routine practice. Remimazolam is often used as a single agent for short-duration surgical sedation due to its rapid onset, fast metabolism, and predictable pharmacokinetic characteristics. In contrast, propofol is the first-line drug for the induction and maintenance of general anesthesia as well as for independent sedation. The combined use of the two is only seen in highly specialized clinical situations (such as dose titration for refractory sedation in a small number of patients), and a standardized dosing regimen has not been established yet. First, the underlying molecular mechanisms may not be limited to the PI3K/AKT pathway; additional pathways involved in the regulatory effects of remimazolam and propofol on BMMSCs require further exploration. Second, remimazolam and propofol may inhibit IL-8 secretion through indirect regulation, which warrants further validation [39, 40]. Collectively, remimazolam and propofol can inhibit the biological functions of BMMSCs either alone or synergistically, with remimazolam exhibiting a milder inhibitory effect compared to propofol; these effects further regulate the progression of gastric cancer cells (**Figure 7**). In conclusion, our findings provide experimental evidence for the rational clinical administration of anesthetics, particularly for patients with gastric cancer undergoing anesthesia.

Acknowledgements

This work was supported by the Zhenjiang Science and Technology Planning Project, Grant/Award Number: SH2024017.

Disclosure of conflict of interest

None.

Abbreviations

BMMSCs, bone marrow mesenchymal stem cells; Pro-BMMSCs-CM, the supernatant of BMMSCs treated with propofol; Rem-BMMSCs-CM, the supernatant of BMMSCs treated with Remimazolam.

Address correspondence to: Wei Zhu, School of Medicine, Jiangsu University, No. 301 Xuefu Road, Zhenjiang 212013, Jiangsu, China. E-mail: zhuwei@ujs.edu.cn; Dr. Jin Wu, Department of Anesthesiology, Affiliated Hospital of Jiangsu University, No. 438 Jie Fang Road, Zhenjiang 212001, Jiangsu, China. E-mail: wujin914@hotmail.com

References

[1] Perico L, Morigi M, Rota C, Breno M, Mele C, Noris M, Introna M, Capelli C, Longaretti L, Rottoli D, Conti S, Corna D, Remuzzi G and Benigni A. Human mesenchymal stromal cells transplanted into mice stimulate renal tubular cells and enhance mitochondrial function. Nat Commun 2017; 8: 983.

[2] Jammes M, Tabasi A, Bach T and Ritter T. Healing the cornea: exploring the therapeutic solutions offered by MSCs and MSC-derived EVs. Prog Retin Eye Res 2024; 105: 101325.

[3] Amsalem Y, Mardor Y, Feinberg MS, Landa N, Miller L, Daniels D, Ocherashvilli A, Holbova R, Yosef O, Barbash IM and Leor J. Iron-oxide labeling and outcome of transplanted mesenchymal stem cells in the infarcted myocardium. Circulation 2007; 116 Suppl: I38-I45.

[4] Naftali-Shani N, Levin-Kotler L-P, Palevski D, Amit U, Kain D, Landa N, Hochhauser E and Leor J. Left ventricular dysfunction switches mesenchymal stromal cells toward an inflammatory phenotype and impairs their reparative properties via toll-like receptor-4. Circulation 2017; 135: 2271-2287.

[5] Chen K, Tao H, Xiao H, Chu M, Zhu P, Lv S, Huang L and Geng D. Identification of ferroptosis/autophagy-related genes and potential underlying mechanisms involved in the effect of BMSC senescence on the osteogenic differentiation of aging BMSCs. Genes Dis 2024; 12: 101259.

[6] Chen B, Yu J, Wang Q, Zhao Y, Sun L, Xu C, Zhao X, Shen B, Wang M, Xu W and Zhu W. Human bone marrow mesenchymal stem cells promote gastric cancer growth via regulating c-Myc. Stem Cells Int 2018; 2018: 9501747.

[7] Wang M, Zhao X, Qiu R, Gong Z, Huang F, Yu W, Shen B, Sha X, Dong H, Huang J, Wang L, Zhu W and Xu W. Lymph node metastasis-derived gastric cancer cells educate bone marrow-derived mesenchymal stem cells via YAP signaling activation by exosomal Wnt5a. Oncogene 2021; 40: 2296-2308.

[8] Zhu W, Huang L, Li Y, Qian H, Shan X, Yan Y, Mao F, Wu X and Xu WR. Mesenchymal stem cell-secreted soluble signaling molecules potentiate tumor growth. Cell Cycle 2011; 10: 3198-3207.

[9] Liu CJ, Kuo FC, Wang CL, Kuo CH, Wang SSW, Chen CY, Huang YB, Cheng KH, Yokoyama KK, Chen CL, Lu CY and Wu DC. Suppression of IL-8-Src signalling axis by 17β-estradiol inhibits human mesenchymal stem cells-mediated gastric cancer invasion. J Cell Mol Med 2016; 20: 962-972.

[10] Keam SJ. Remimazolam: first approval. Drugs 2020; 80: 625-633.

[11] Lee A and Shirley M. Remimazolam: a review in procedural sedation. Drugs 2021; 81: 1193-1201.

[12] Wang X, Liu Y, Zhang S, Zheng L, Kang Y, Sheng P and Zhang Z. Aspirin attenuates the detrimental effects of TNF-α on BMMSC stemness by modulating the YAP-SMAD7 axis. Mol Med 2024; 30: 126.

[13] Holan V, Cechova K, Zajicova A, Kossl J, Hermankova B, Bohacova P, Hajkova M, Krulova M, Svoboda P and Javorkova E. The impact of morphine on the characteristics and function properties of human mesenchymal stem cells. Stem Cell Rev Rep 2018; 14: 801-811.

[14] Li Q, Liu T, Zhang L, Liu Y, Zhang W, Liu W, Cao Y and Zhou G. The role of bFGF in down-regulating α-SMA expression of chondrogenically induced BMSCs and preventing the shrinkage of BMSC engineered cartilage. Biomaterials 2011; 32: 4773-4781.

[15] Zhou YH, Li SX, Li L, Deng CM, Shen JJ, Wang DX, Chen XZ and Xu LL. Effect of remimazolam supplementation on propofol requirements during hysteroscopy: a double-blind, dose-response study. Anesth Analg 2024; 139: 1309-1316.

[16] Shimizu T, Takasusuki T and Yamaguchi S. Remimazolam compared to propofol for total intravenous anesthesia with remifentanil on the recovery of psychomotor function: a randomized controlled trial. Adv Ther 2023; 40: 4395-4404.

[17] Jung Y, Kim JK, Shiozawa Y, Wang J, Mishra A, Joseph J, Berry JE, McGee S, Lee E, Sun H, Wang J, Jin T, Zhang H, Dai J, Krebsbach PH, Keller ET, Pienta KJ and Taichman RS. Recruitment of mesenchymal stem cells into prostate tumours promotes metastasis. Nat Commun 2013; 4: 1795.

[18] Li W, Zhang X, Wu F, Zhou Y, Bao Z, Li H, Zheng P and Zhao S. Gastric cancer-derived mesenchymal stromal cells trigger M2 macrophage polarization that promotes metastasis and EMT in gastric cancer. Cell Death Dis 2019; 10: 918.

[19] Karnoub AE, Dash AB, Vo AP, Sullivan A, Brooks MW, Bell GW, Richardson AL, Polyak K, Tubo R and Weinberg RA. Mesenchymal stem cells within tumour stroma promote breast cancer metastasis. Nature 2007; 449: 557-563.

[20] Zhu W, Huang L, Li Y, Zhang X, Gu J, Yan Y, Xu X, Wang M, Qian H and Xu W. Exosomes derived from human bone marrow mesenchymal stem cells promote tumor growth in vivo. Cancer Lett 2011; 315: 28-37.
[21] Xu L, Hou X, Zhou X and Jiang M. Advances in the research and application of stem cell therapies for idiopathic pulmonary fibrosis. Am J Clin Exp Immunol 2025; 14: 300-312.
[22] Masui K. Remimazolam besilate, a benzodiazepine, has been approved for general anesthesia! J Anesth 2020; 34: 479-482.
[23] Chen X, Sang N, Song K, Zhong W, Wang H, Jiang J, Huang Y and Hu P. Psychomotor recovery following remimazolam-induced sedation and the effectiveness of flumazenil as an antidote. Clin Ther 2020; 42: 614-624.
[24] Hu Q, Liu X, Wen C, Li D and Lei X. Remimazolam: an updated review of a new sedative and anaesthetic. Drug Des Devel Ther 2022; 16: 3957-3974.
[25] Jiang S, Liu Y, Huang L, Zhang F and Kang R. Effects of propofol on cancer development and chemotherapy: potential mechanisms. Eur J Pharmacol 2018; 831: 46-51.
[26] Tang Y, Yang X, Yu Y, Shu H, Yuan Y, Liu H, Zou X, Yuan S and Shang Y. Remimazolam besylate versus propofol for long-term sedation during invasive mechanical ventilation: a pilot study. Crit Care 2022; 26: 279.
[27] Choi JY, Lee HS, Kim JY, Han DW, Yang JY, Kim MJ and Song Y. Comparison of remimazolam-based and propofol-based total intravenous anesthesia on postoperative quality of recovery: a randomized non-inferiority trial. J Clin Anesth 2022; 82: 110955.
[28] Hu C, Wang B, Liu Z, Chen Q, Ishikawa M, Lin H, Lian Q, Li J, Li JV and Ma D; ESA-IC Onco-Anaesthesiology Research Group. Sevoflurane but not propofol enhances ovarian cancer cell biology through regulating cellular metabolic and signaling mechanisms. Cell Biol Toxicol 2022; 39: 1395-1411.
[29] Bowling AC and DeLorenzo RJ. Micromolar affinity benzodiazepine receptors: identification and characterization in central nervous system. Science 1982; 216: 1247-1250.
[30] Wang N, Shen X, Huang H, Zhao R, Jiwa H, Li Z, Li P, Ye J and Zhou Q. The bidirectional effects of APPswe on the osteogenic differentiation of MSCs in bone homeostasis by regulating notch signaling. Genes Dis 2024; 12: 101317.
[31] Teng CF, Jeng LB and Shyu WC. Role of insulin-like growth factor 1 receptor signaling in stem cell stemness and therapeutic efficacy. Cell Transplant 2018; 27: 1313-1319.
[32] Ma Q, Chen G, Li Y, Guo Z and Zhang X. The molecular genetics of PI3K/PTEN/AKT/mTOR pathway in the malformations of cortical development. Genes Dis 2023; 11: 101021.
[33] He Y, Sun MM, Zhang GG, Yang J, Chen KS, Xu WW and Li B. Targeting PI3K/Akt signal transduction for cancer therapy. Signal Transduct Target Ther 2021; 6: 425.
[34] Yu L, Wei J and Liu P. Attacking the PI3K/Akt/mTOR signaling pathway for targeted therapeutic treatment in human cancer. Semin Cancer Biol 2021; 85: 69-94.
[35] Lin HY, Wang WK, Lin CH, Kuei CH, Lee HH, Kent Lin YH, Chiu HW and Lin YF. The IL-8/NF-κB feedback loop confers a paclitaxel-sensitive/doxorubicin-resistant phenotype in triple-negative breast cancer. Free Radic Biol Med 2025; 238: 316-328.
[36] Jorgensen C and Khoury M. Musculoskeletal progenitor/stromal cell-derived mitochondria modulate cell differentiation and therapeutical function. Front Immunol 2021; 12: 606781.
[37] Fousek K, Horn LA and Palena C. Interleukin-8: a chemokine at the intersection of cancer plasticity, angiogenesis, and immune suppression. Pharmacol Ther 2020; 219: 107692.
[38] Zhu Q, Wei X, Qu Z, Lu L, Zhang Y and Wang H. The roles of cell cycle proteins in regulating the tumor immune microenvironment. Genes Dis 2025; 13: 101706.
[39] Aggarwal S, Goyal VK, Chaturvedi SK, Mathur V, Baj B and Kumar A. A comparative study between propofol and etomidate in patients under general anesthesia. Braz J Anesthesiol 2015; 66: 237-241.
[40] Sneyd JR and Rigby-Jones AE. Remimazolam for anaesthesia or sedation. Curr Opin Anaesthesiol 2020; 33: 506-511.